Letter

Heat capacity of $URu_{2-x}Os_xSi_2$ at low temperatures

D. L. Kunwar,[1] S. R. Panday,[1] Y. Deng,[2,3] S. Ran,[4] R. E. Baumbach,[5,6]
M. B. Maple,[2,3] Carmen C. Almasan,[1] and M. Dzero[1]

[1]*Department of Physics, Kent State University, Kent, Ohio 44242, USA*
[2]*Center for Advanced Nanoscience, University of California, San Diego, La Jolla, California 92093, USA*
[3]*Department of Physics, University of California, San Diego, La Jolla, California 92903, USA*
[4]*Department of Physics, Washington University in St. Louis, St. Louis, Missouri 63130, USA*
[5]*National High Magnetic Field Laboratory, Florida State University, Tallahassee, Florida 32310, USA*
[6]*Department of Physics, Florida State University, Tallahassee, Florida 32306, USA*

(Received 19 October 2021; accepted 3 January 2022; published 13 January 2022)

We perform measurements of the heat capacity as a function of temperature on $URu_{2-x}Os_xSi_2$ alloys. Our experimental results show that the critical temperature of the second-order phase transition increases while the value of the Sommerfeld coefficient in the ordered state decreases with an increase in osmium concentration. We also observe an increase in the values of the heat capacity at the critical temperature as well as a broadening of the critical fluctuation region with an increase in x. We analyze the experimental data using the Haule-Kotliar model which, in particular, identifies the "hidden order" transition in the parent material URu_2Si_2 as a transition to a state with a nonzero hexadecapole moment. We demonstrate that our experimental results are consistent with the predictions of that model.

DOI: 10.1103/PhysRevB.105.L041106

I. INTRODUCTION

The manifestly second-order phase transition develops in URu_2Si_2 at temperature $T_{c0} = 17.55$ K [1–4]. The nature of the order parameter emerging below the transition has remained hotly debated for the last 25 years [5–10]. In particular, the problem with the identification of the order parameter has made an analysis of thermodynamic data quite challenging. Notably, the temperature dependence of the heat capacity, for example, shows that the Ginzburg region, where the contribution from critical fluctuations is comparable to or exceeds the mean-field contribution, is very narrow, and yet the absence of a clear idea about the nature of the order parameter inhibits any attempt to analyze the thermodynamic data even at the mean-field level.

Despite the fact that significant progress was made both experimentally and theoretically towards the identification of the "hidden order" [9,10], new ideas about the nature of the hidden order transition still continue to appear [11–18]. Specifically, one of the main focus points of the ongoing discussions is still whether the hidden order transition involves quasilocalized $5f^2$ states of uranium or is driven by the itinerant electronic degrees of freedom, which are hybridized with the $5f$ electronic states. The possible resolution of this debate is likely to come from designing the experiments in a way that would help one to unambiguously contrast the measurement results with theoretical predictions [19–22].

One type of such experiments involves the study of alloys in which Ru is substituted with either Fe or Os [23–25]. For example, the substitution of Ru with Os produces an effect of negative pressure, leading to a predominantly isotropic lattice expansion. By contrasting the changes in the critical temperature T_c with the changes in the Sommerfeld coefficient γ, one should (at least, in principle) be able to check whether this leads to a contradiction to either "itinerant" or "localized" theoretical models. Qualitatively, in the itinerant scenario, for example, one would expect that both γ and T_c should either decrease or increase with the change in external pressure since both of these quantities provide a measure of hybridization between the itinerant and localized degrees of freedom.

In this Letter, we report on the measurements of the heat capacity in $URu_{2-x}Os_xSi_2$ across the hidden order phase transition. Our experimental results demonstrate that the critical temperature of the transition grows with an increase in osmium concentration and reaches a value of $T_c \approx 1.43T_{c0}$ for $x = 0.2$ (see Fig. 1). Consequently, we have also analyzed the electronic contribution to the heat capacity at low enough temperatures below T_c and found that the Sommerfeld coefficient actually decreases with x. We were also able to obtain satisfactory fits for the heat capacity data using the model put forward by Haule and Kotliar [11,26], which explains the second-order transition as a state with a complex order parameter: the real part of the order parameter corresponds to the nonzero hexadecapole moment, while the imaginary part is determined by the staggered magnetic moment. Taking into account the results of the earlier transport measurements in $URu_{2-x}Os_xSi_2$, we arrived at the conclusion that osmium substitutions promote the emergence of the antiferromagnetic order at concentrations $x \geqslant 0.15$.

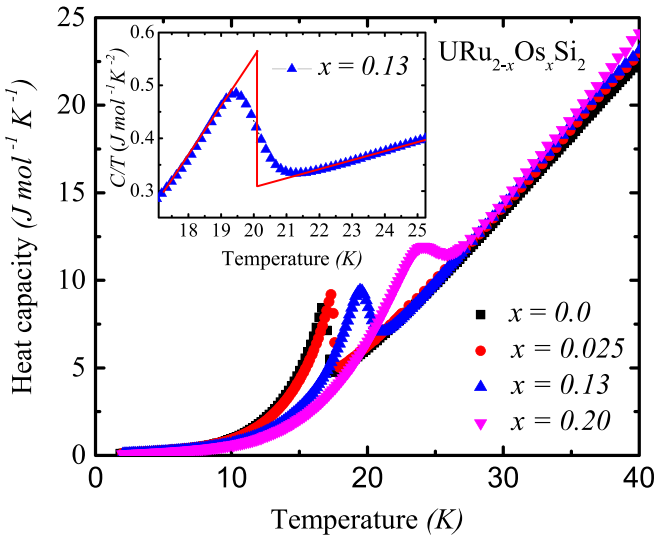

FIG. 1. Heat capacity C as a function of temperature T in $URu_{2-x}Os_xSi_2$ alloys. Inset: Entropy construction to estimate the critical temperature of the second-order phase transition. There are three main features that are of interest to us: the critical temperature T_c, the maximum value of the heat capacity, and the broadening of the thermal fluctuation region around T_c all increase with increasing osmium concentration x.

II. EXPERIMENTAL DETAILS

Single crystals of $URu_{2-x}Os_xSi_2$ were grown using the Czochralski method in a tetra-arc furnace. The crystals were cut into a rectangle with the c axis along the shortest dimension of the crystal. These single crystals were first polished with sandpaper to make their surface smooth for better coupling to the heat capacity platform. They were then washed thoroughly with ethanol to remove any impurities left. In this paper we quote the actual values of osmium concentrations.

Heat capacity measurements were performed in zero magnetic field over the temperature range $T = 2$–50 K, and the data were obtained using a relaxation technique in the He-4 option of the Quantum Design physical properties measurement system.

III. DATA ANALYSIS

The analysis of the heat capacity data at temperatures much lower than the critical temperature, $T \ll T_c$, is straightforward since the main contribution to the heat capacity in this temperature region comes from itinerant electrons and lattice vibrations, $C_{\rm el}(T) + C_{\rm ph}(T)$. We find that at low temperatures $C_{\rm el}(T) \approx \gamma T$ and $C_{\rm ph}(T) = (T/\omega_D)^3 \mathcal{I}(\omega_D/T)$, where γ is the Sommerfeld coefficient, ω_D is the Debye temperature, and $\mathcal{I}(x)$ is a known function of x: $\mathcal{I}(x \to \infty) \approx 26$.

At temperatures $T \sim T_c$, however, the contribution from the electronic degrees of freedom, which govern the hidden order transition, becomes a dominant one. In order to analyze our data in this temperature region, one generally needs to put forward an idea about the origin of the order parameter so that the temperature dependence of the heat capacity can be computed and, ultimately, can be compared to (or used to fit) the experimental data. Thus, as a starting point, we need to decide whether to consider the itinerant degrees of freedom (i.e., electrons on the *spd* orbitals of uranium) as a driving force for the second-order phase transition or, on the contrary, adopt the "localized picture" in which the electrons on the localized $5f^2$ orbitals are the main driving force for the transition. Based on earlier observations of BCS-like features of the transition in the stoichiometric URu_2Si_2 [1], it is, indeed, tempting to use one of the recently proposed itinerant models (for a recent review see [9] and references therein) to analyze the data. One needs to keep in mind, however, that the mean-field-like temperature dependence of the thermodynamic response functions in the BCS model [27] (excluding the very narrow region in the immediate vicinity of the transition) is controlled by the retarded nature of the electron-phonon interactions that drive the superconducting transition [28]. This is manifested in the smallness of the ratio of the Debye frequency to the Fermi energy, $\omega_D/\varepsilon_F \ll 1$ [29,30]. In particular, in the weak-coupling limit, the retardation effects are implemented as an ultraviolet cutoff $\Lambda = \omega_D$ in the self-consistent calculation of the order parameter. There are known limitations to this line of arguments [31], but we think that these limitations are not relevant for the hidden order transition. To summarize, to the best of our knowledge there is no experimental evidence for the retardation effects being observed through the hidden order transition and the emergence of an energy scale (analogous to ω_D in the BCS theory) that would be much smaller than the Fermi energy.

Therefore, we are compelled to adopt a point of view in which interactions between the localized f-orbital degrees of freedom must be the ones leading to the transition [32]. Among the multiple models available to us (see, e.g., [9,10] for review) to analyze our data we consider the model proposed by Haule and Kotliar (HK) [11,26]. The HK model involves a system of interacting two-level systems (TLSs), and each TLS corresponds to a ground-state non-Kramers doublet of the uranium $5f^2$ valence configuration. The components of the corresponding state vector $|\Psi\rangle^T = (|a\rangle\ |b\rangle)$ of the non-Kramers doublet are

$$|a\rangle = \frac{i}{\sqrt{2}}(|4\rangle - |-4\rangle),$$
$$|b\rangle = \frac{\cos\phi}{\sqrt{2}}(|4\rangle + |-4\rangle) - \sin\phi|0\rangle.$$

Here the states are written in the eigenbasis of the total angular momentum operator $\hat{J}^2$ and its projection on the z axis $\hat{J}_z$ (we remind the reader that the $5f^2$ valence configuration corresponds to a state with $J = 4$). One can check that the following averages acquire nonzero values: $\langle b|\hat{J}_z|a\rangle = 4i\cos\phi$ and $\langle b|(\hat{J}_x\hat{J}_y + \hat{J}_y\hat{J}_x)(\hat{J}_x^2 - \hat{J}_y^2)|a\rangle = 12\sqrt{35}\sin\phi + 28\cos\phi$. Here ϕ is a parameter that ultimately determines the magnitude of the magnetic moment at $T \ll T_c(x = 0)$ in the hidden order state. Thus, it is convenient to formally associate the first average with $\langle\Psi|\hat{\sigma}_y|\Psi\rangle$ and the second average with $\langle\Psi|\hat{\sigma}_x|\Psi\rangle$, where $\hat{\sigma}_x$ and $\hat{\sigma}_y$ are the Pauli matrices. As a result, one can formally introduce the complex order parameter $\psi = \langle\Psi|\hat{\sigma}_x + i\hat{\sigma}_y|\Psi\rangle$ describing a state that may emerge below some temperature as the lowest-energy

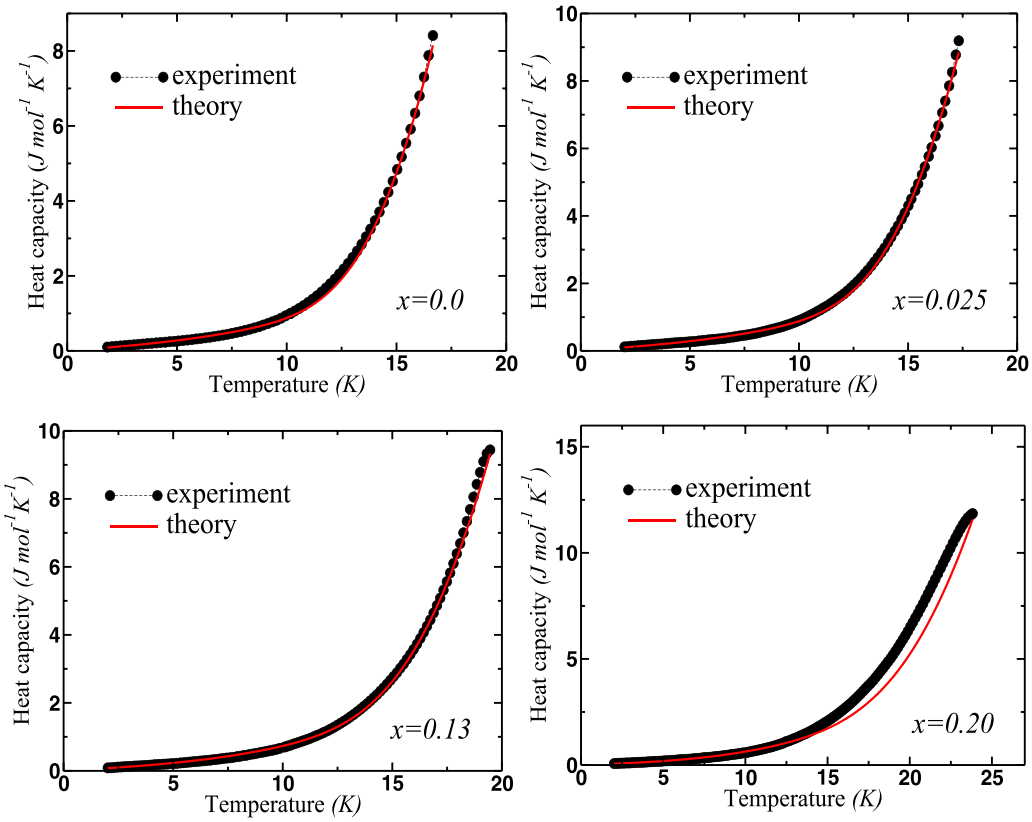

FIG. 2. Results of our analysis of the heat capacity at temperatures below the critical temperature. To fit the data in the panel for $x = 0$, we used the following values of the parameters: $n_{\rm ph} = 375$, $n_{\rm tls} = 9.15$, $\gamma = 0.049$ (J/mol K^2), $\omega_D = 305$ K, $V_0 = 18.25$ K, and $s(T = 0) = 3.85$. To fit the remaining data, we changed only the values of γ and V_0. In the panel for $x = 0.025$, $\gamma = 0.049$ (J/mol K^2), $V_0 = 18.75$. In the panel for $x = 0.13$, $\gamma = 0.038$ (J/mol K^2), $V_0 = 21.15$. In the panel for $x = 0.20$, $\gamma = 0.029$ (J/mol K^2), $V_0 = 25.75$ K.

state for the following Hamiltonian:

$$\hat{H} = -\sum_{i\neq j} V(\vec{r}_i - \vec{r}_j)\hat{\sigma}_x(\vec{r}_i)\hat{\sigma}_x(\vec{r}_j) - \frac{\Delta}{2}\sum_i \hat{\sigma}_z(\vec{r}_i) + \sum_{ij} U(\vec{r}_i - \vec{r}_j)\hat{\sigma}_y(\vec{r}_i)\hat{\sigma}_y(\vec{r}_j). \quad (1)$$

Here the first term describes the interactions which lead to the emergence of the hidden order ($V > 0$, a state with nonzero hexadecapole moment), the second term accounts for the splitting of the non-Kramers doublet, and the third term accounts for the antiferromagnetic interactions ($U > 0$). As was recently shown [26], the mean-field analysis of the model Hamiltonian (1) provides a satisfactory description of the thermodynamics measurements under external pressure and magnetic field.

To perform the data analysis, we introduce several simplifications of the model Hamiltonian (1). First and foremost we assume that the interactions leading to the emergence of the nonzero expectation value $\langle\Psi|\hat{\sigma}_x|\Psi\rangle$ are sufficiently long range, with the characteristic length scale $r_0 \gg a$ (a is the lattice spacing). This allows us to perform a controlled calculation of the heat capacity, so that the contribution from thermal fluctuation effects is small in powers of $(a/r_0)^3$ [33]. Second, we completely neglect the contribution from the last two terms: the second term is practically irrelevant for the temperatures $T \sim T_c$, while, as we will see from our analysis below, the third term contributes significantly to the heat capacity only at relatively high osmium concentrations, $x \sim 15\%$.

In order to compute the specific heat, we follow the avenue of Ref. [33]. We introduce $s = \langle\Psi|\hat{\sigma}_x(\vec{r}_i)|\Psi\rangle$, and following our discussion above, we rewrite (1) as follows:

$$\hat{H} = NV_0s^2 - sV_0\sum_i \hat{\sigma}_x(\vec{r}_j) - \sum_{i\neq j} V(\vec{r}_i - \vec{r}_j)(\hat{\sigma}_x(\vec{r}_i) - s)(\hat{\sigma}_x(\vec{r}_j) - s), \quad (2)$$

where $V_0 = \sum_j V(\vec{r}_i - \vec{r}_j)$ and N is the number of uranium lattice sites. Within the mean-field approximation the third term in (2) can be neglected as it describes the effect of thermal fluctuations on the mean-field results. The subsequent minimization of the free energy with respect to the mean-field parameter s ultimately results in the following expression for the heat capacity ($k_B = 1$, $\beta = 1/T$):

$$c_{\rm h.o.}(T) = \frac{(\beta V_0 s(T))^2}{\cosh^2[\beta V_0 s(T)] - \beta V_0}, \quad (3)$$

and the temperature dependence of the order parameter $s(T)$ can be found by solving the mean-field equation $s = \tanh(\beta V_0 s)$.

Thus, we write $C(T) = C_{\rm el}(T) + C_{\rm ph}(T) + C_{\rm h.o.}(T)$ and employ this expression to fit our heat capacity data. Specifically, we use the data for the stoichiometric compound to

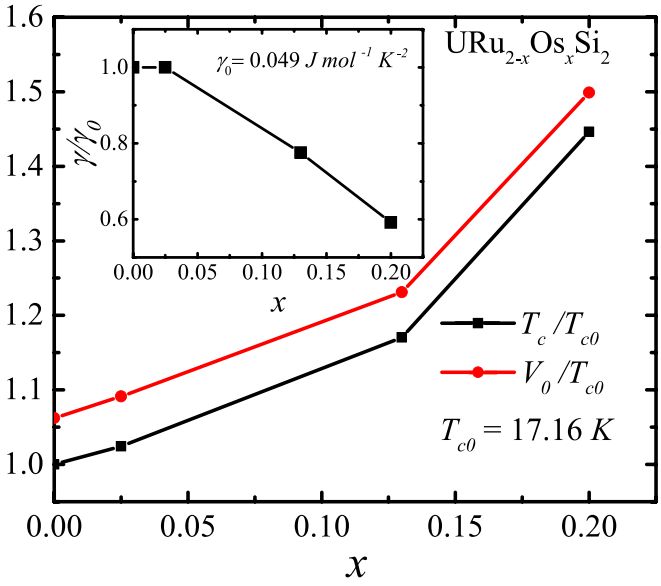

FIG. 3. Dependence of the interaction strength V_0 and the critical temperature of the second phase transition as a function of osmium concentration x. Given the overall mean-field nature of the transition, it is not surprising to find $V_0 \propto T_c$. Inset: Extracted value of the Sommerfeld coefficient γ as a function of the osmium concentration x. The reduction in the value of γ signals a decrease in the hybridization between the spd- and f-electron states of uranium.

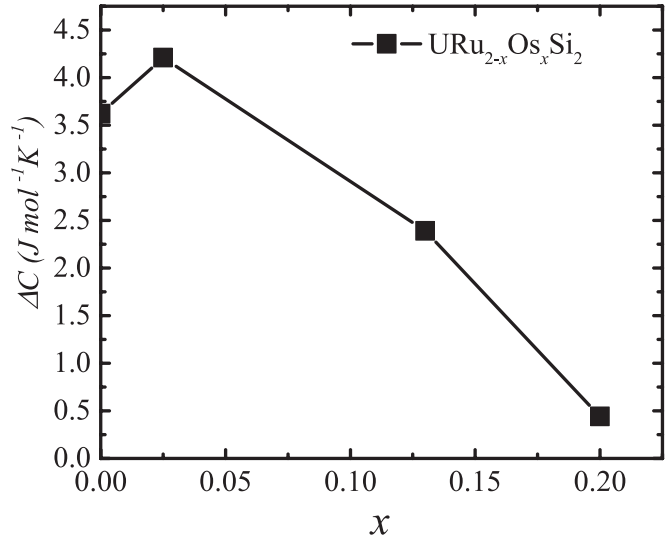

FIG. 4. Specific heat jump at the critical temperature, $\Delta C(T_c) = C_{\max}(T_c - \epsilon) - C_{\min}(T_c + \epsilon)$ ($\epsilon \ll T_c$), as a function of osmium concentration x.

find the corresponding prefactors for the phonon, $C_{\rm ph}(T) = n_{\rm ph} c_{\rm ph}(T)$, and f-electron, $C_{\rm h.o.}(T) = n_{\rm tls} c_{\rm h.o.}(T)$, contributions along with the Debye temperature ω_D and dimensionless matrix element $s(T = 0)$. We note here that for the case of higher concentrations, $x > 15\%$, the mean-field order parameter introduced above should be understood as an absolute value of the matrix element $\langle\Psi|[\hat{\sigma}_x(\vec{r}_i) + i\hat{\sigma}_y(\vec{r}_i)]|\Psi\rangle$.

The results of our analysis are shown in Fig. 2. Generally, we find that the heat capacity data for $x = 0$, $x = 0.025$, and $x = 0.13$ can be systematically described by our model (2). After we find a satisfactory result by fixing the lattice parameters obtained from the analysis of the heat capacity data at $T \leqslant T_c$ for URu_2Si_2, we analyze the remaining sets by changing only two parameters: the interaction strength V_0 and Sommerfeld coefficient γ.

Since we have observed experimentally that the critical temperature of the transition increases with x and also because, at the level of the mean-field approximation, $T_c \simeq V_0$, it follows that in order to obtain good fits to the data we need to increase the value of V_0. At the same time we have also noted that the best fits are obtained if we gradually decrease the value of γ while increasing x. These results are summarized in Fig. 3.

Our fitting procedure did not work well for the $x = 0.2$ sample: there are obvious discrepancies between the theoretically predicted result and the experimental data in the temperature region where the contribution from the f electrons becomes comparable with the remaining contributions from the itinerant electrons and the lattice vibrations. Our interpretation of these observations is discussed in what follows.

IV. DISCUSSION

The possible origin of the discrepancy between the results of our fitting procedure and the heat capacity for $x = 0.2$ can be traced back to the recent results of transport studies of $URu_{2-x}Os_xSi_2$ [23]. Specifically, it was shown that at approximately $x \approx 0.15$ there is a change in slope of T_c vs x corresponding to the onset of the long-range antiferromagnetic order. In addition, we note that the value of the heat capacity for $x = 0.2$ at $T = T_c$ exceeds the corresponding values for other samples by approximately 20%. This fact can be accounted for by the enhanced exchange interactions $U(\vec{r}_i - \vec{r}_j)$. In addition, our data clearly show that there is an increasing contribution $\propto (a/r_0)^3\sqrt{T_c/|T - T_c|}$ from the thermally induced magnetic fluctuations with the correlation function $D_{ij} = \langle[\hat{\sigma}_y(\vec{r}_i) - \mu_s][\hat{\sigma}_y(\vec{r}_j) - \mu_s]\rangle$, where μ_s is the value of the staggered magnetic moment. These observations are supported by the decrease of the specific heat jump at $T = T_c$ (Fig. 4), which is again accounted for by the broadening of the Ginzburg region, which we estimate to be $|\delta T|/T_c \simeq (a/r_0)^6$. In other words, the expansion of the lattice with x must cause the reduction of r_0 and the broadening of the critical fluctuation region.

Another consequence of our analysis is the observation of the decreasing value of the Sommerfeld coefficient $\gamma(x)$ with x (Fig. 3, inset). This reduction most likely is induced by the diminished hybridization between the spd and $5f^2$ states. Since the effect of osmium substitution produces the lattice expansion, the reduction in hybridization implies that the leading fluctuation channel is $5f^2 \leftrightarrow 5f^1$, as was suggested in Ref. [18]. This behavior is in contrast to the option of valence fluctuations in the second channel $5f^2 \leftrightarrow 5f^3$, which would actually be enhanced with an increase in x and, consequently, would lead to an increase in the values of γ.

Last, we would like to comment on the increasing value of V_0 which follows from our fitting procedure. We remind the reader that the parameter V_0 plays the role of the effective

interaction strength and is equal to $V(\mathbf{r})$ integrated over space, Eq. (2). Earlier studies [1,24,25,34] have associated the product $V_0 s(0)$ with the hybridization (and/or charge) gap. In our theory $s(0)$ cannot possibly change with x or external pressure since its value is determined by a local matrix element. However, since the lattice is expanding, V_0 must be changing, and its apparent increase with x implies that V_0 must be inverse proportional to the correlation radius r_0.

V. CONCLUSIONS

We have measured and analyzed the heat capacity as a function of temperature in $URu_{2-x}Os_xSi_2$. Osmium alloying leads to a lattice expansion equivalent to an effect of negative pressure. Our data may be considered an addition to the transport data on the same alloys [23], with similar conclusions regarding the increase in T_c with x. Decreasing values of the Sommerfeld coefficient with the increase in x implies that the second-order phase transition is driven by the interactions between the localized f-orbital degrees of freedom. The second important aspect of our work consists of an attempt to use a theoretical model to analyze our results: this is in clear contrast to earlier experimental studies which used purely phenomenological expressions [1,23–25,34] to estimate the changes in the heat capacity through the second-order transition.

ACKNOWLEDGMENTS

The work at Kent State University was financially supported by the National Science Foundation (NSF) under Grants No. DMR-1904315 (D.L.K. and C.C.A.) and No. NSF-DMR-2002795 (S.R.P. and M.D.). Research at the University of California, San Diego, was supported by the U.S. Department of Energy (DOE), Office of Science, Basic Energy Sciences (BES), under Grant No. DE-FG02-04ER46105 (single-crystal growth) and by the NSF under Grant No. DMR-1810310 (physical properties measurements). Research at the National High Magnetic Field Laboratory was supported by NSF Cooperative Agreement No. DMR-1157490, the state of Florida, and the DOE. R.E.B. was supported by the Center for Actinide Science and Technology (CAST), an Energy Frontier Research Center (EFRC) funded by the U.S. DOE, BES, under Grant No. DE-SC0016568.

[1] T. T. M. Palstra, A. A. Menovsky, J. van den Berg, A. J. Dirkmaat, P. H. Kes, G. J. Nieuwenhuys, and J. A. Mydosh, Phys. Rev. Lett. **55**, 2727 (1985).
[2] M. B. Maple, J. W. Chen, Y. Dalichaouch, T. Kohara, C. Rossel, M. S. Torikachvili, M. W. McElfresh, and J. D. Thompson, Phys. Rev. Lett. **56**, 185 (1986).
[3] W. Schlabitz, J. Baumann, B. Pollit, U. Rauchschwalbe, H. M. Mayer, U. Ahlheim, and C. D. Bredl, Z. Phys. B **62**, 171 (1986).
[4] C. Broholm, J. K. Kjems, W. J. L. Buyers, P. Matthews, T. T. M. Palstra, A. A. Menovsky, and J. A. Mydosh, Phys. Rev. Lett. **58**, 1467 (1987).
[5] V. Barzykin and L. P. Gor'kov, Phys. Rev. Lett. **74**, 4301 (1995).
[6] H. Ikeda and Y. Ohashi, Phys. Rev. Lett. **81**, 3723 (1998).
[7] N. Shah, P. Chandra, P. Coleman, and J. A. Mydosh, Phys. Rev. B **61**, 564 (2000).
[8] P. Chandra, P. Coleman, J. A. Mydosh, and V. Tripathi, Nature (London) **417**, 831 (2002).
[9] J. Mydosh, Philos. Mag. **94**, 3640 (2014).
[10] J. A. Mydosh, P. M. Oppeneer, and P. S. Riseborough, J. Phys.: Condens. Matter **32**, 143002 (2020).
[11] K. Haule and G. Kotliar, Nat. Phys. **5**, 796 (2009).
[12] P. Kotetes and G. Varelogiannis, Phys. Rev. Lett. **104**, 106404 (2010).
[13] Y. Dubi and A. V. Balatsky, Phys. Rev. Lett. **106**, 086401 (2011).
[14] C. Pépin, M. R. Norman, S. Burdin, and A. Ferraz, Phys. Rev. Lett. **106**, 106601 (2011).
[15] S. Fujimoto, Phys. Rev. Lett. **106**, 196407 (2011).
[16] P. S. Riseborough, B. Coqblin, and S. G. Magalhães, Phys. Rev. B **85**, 165116 (2012).
[17] C.-H. Hsu and S. Chakravarty, Phys. Rev. B **87**, 085114 (2013).
[18] P. Chandra, P. Coleman, and R. Flint, Nature (London) **493**, 621 (2013).
[19] J. R. Jeffries, K. T. Moore, N. P. Butch, and M. B. Maple, Phys. Rev. B **82**, 033103 (2010).
[20] W. K. Park, P. H. Tobash, F. Ronning, E. D. Bauer, J. L. Sarrao, J. D. Thompson, and L. H. Greene, Phys. Rev. Lett. **108**, 246403 (2012).
[21] X. Lu, F. Ronning, P. H. Tobash, K. Gofryk, E. D. Bauer, and J. D. Thompson, Phys. Rev. B **85**, 020402(R) (2012).
[22] H.-H. Kung, R. E. Baumbach, E. D. Bauer, V. K. Thorsmølle, W.-L. Zhang, K. Haule, J. A. Mydosh, and G. Blumberg, Science **347**, 1339 (2015).
[23] C. T. Wolowiec, N. Kanchanavatee, K. Huang, S. Ran, A. J. Breindel, N. Pouse, K. Sasmal, R. E. Baumbach, G. Chappell, P. S. Riseborough *et al.*, Proc. Natl. Acad. Sci. USA **118** e2026591118 (2021).
[24] S. Ran, C. T. Wolowiec, I. Jeon, N. Pouse, N. Kanchanavatee, B. D. White, K. Huang, D. Martien, T. DaPron, D. Snow *et al.*, Proc. Natl. Acad. Sci. USA **113**, 13348 (2016).
[25] S. Ran, I. Jeon, N. Pouse, A. J. Breindel, N. Kanchanavatee, K. Huang, A. Gallagher, K.-W. Chen, D. Graf, R. E. Baumbach *et al.*, Proc. Natl. Acad. Sci. USA **114**, 9826 (2017).
[26] K. Haule and G. Kotliar, Europhys. Lett. **89**, 57006 (2010).
[27] J. Bardeen, L. N. Cooper, and J. R. Schrieffer, Phys. Rev. **108**, 1175 (1957).
[28] G. M. Eliashberg, Pis'ma Zh. Eksp. Teor. Phys. **45**, 28 (1987).
[29] S. Kos, A. J. Millis, and A. I. Larkin, Phys. Rev. B **70**, 214531 (2004).
[30] S. Fischer, M. Hecker, M. Hoyer, and J. Schmalian, Phys. Rev. B **97**, 054510 (2018).
[31] M. Hoyer and J. Schmalian, Phys. Rev. B **97**, 224423 (2018).
[32] P. Shen and M. Dzero, Phys. Rev. B **98**, 125131 (2018).
[33] V. G. Vaks, A. I. Larkin, and S. A. Pikin, Sov. Phys. JETP **24**, 240 (1967).
[34] P. Das, N. Kanchanavatee, J. S. Helton, K. Huang, R. E. Baumbach, E. D. Bauer, B. D. White, V. W. Burnett, M. B. Maple, J. W. Lynn, and M. Janoschek, Phys. Rev. B **91**, 085122 (2015).